Journal of Sustainability, Policy, and Practice
EISSN: 3105-1448 | PISSN: 3105-143X | Vol. 2, No. 1 (2026)

Article

Comparative Evaluation of Machine Learning Algorithms for Spectrophotometric Dental Shade Classification

Pei-ting Chung [1,*]

[1] Department of Chemical and Biomolecular Engineering, University of California, Irvine, USA
* Correspondence: Pei-ting Chung, Department of Chemical and Biomolecular Engineering, University of California, Irvine, USA

Abstract: Accurate dental shade matching is critical for achieving optimal esthetic outcomes in restorative dentistry. This study presents a comparative evaluation of machine learning algorithms for spectrophotometric dental shade classification, focusing on Support Vector Machine, Random Forest, and Extreme Learning Machine approaches. Spectral reflectance data from 1,280 standardized dental composite specimens (as controlled surrogates for shade-guide categories) across 16 VITA Classical shades were collected using a calibrated spectrophotometer. Feature extraction methods, including CIELAB coordinates, spectral coefficients, and principal component analysis, were systematically compared. Experimental results demonstrate that the Extreme Learning Machine achieved the highest classification accuracy of 97.8%; its mean ΔE00 was 1.42, and 89.3% of predictions fell below the clinical acceptability threshold of ΔE00 = 1.8, with a b coordinate RMSE of 2.14. Random Forest demonstrated superior robustness in edge-shade classification, achieving 94.2% accuracy. The findings provide practical guidance for selecting algorithms in industrial dental shade-matching applications.

Keywords: dental shade matching; machine learning; spectrophotometric classification; CIEDE2000

1. Introduction

1.1. Background of Dental Shade Matching

1.2. Clinical Significance of Accurate Shade Selection

Selecting an appropriate dental restoration shade is one of the most challenging aspects of esthetic dentistry. Patient satisfaction with dental restorations depends heavily on the color harmony between artificial materials and natural dentition. Studies indicate that shade mismatch constitutes the primary reason for patient dissatisfaction and restoration replacement, accounting for approximately 35% of esthetic failures in clinical practice.

Dental composite materials exhibit complex optical properties, including translucency, opalescence, and fluorescence, that interact with incident light in ways that differ fundamentally from natural tooth structure. The human eye can detect color differences as small as ΔE = 1.0 under controlled conditions, making precise shade matching essential for clinical success.

1.3. Limitations of Conventional Assessment Methods

Conventional shade-matching procedures involve comparing dental shade guides to the patient's dentition under standardized lighting conditions. Observer fatigue, color vision deficiencies, and variations in ambient lighting contribute to low inter-operator agreement for purely visual assessment methods [1]. Spectrophotometric instruments have emerged as objective alternatives, providing quantitative color measurements based on spectral reflectance analysis across the visible spectrum from 400 to 700 nanometers.

Received: 15 January 2026
Revised: 11 March 2026
Accepted: 24 March 2026
Published: 31 March 2026

1.4. Development of Digital Shade Matching Technologies

Spectrophotometric Measurement Principles

Spectrophotometers quantify tooth color by illuminating the target surface with controlled light and measuring reflected intensity across multiple wavelengths. Modern dental spectrophotometers achieve measurement repeatability with standard deviations below $\Delta E = 0.3$, substantially outperforming visual assessment methods [2]. CIELAB color space represents colors using three coordinates: L for lightness, a for the red--green axis, and b for the yellow--blue axis.

Machine Learning Applications in Dental Color Analysis

Machine learning algorithms have demonstrated significant potential for dental shade classification tasks. Supervised learning approaches can identify complex patterns in spectrophotometric data that correlate with shade guide categories [3]. Classification algorithms, including Support Vector Machines, Random Forests, and neural network architectures, have achieved accuracy rates exceeding 95% in shade prediction tasks under controlled laboratory conditions.

Current Challenges and Research Gaps

Despite advances in digital shade matching technology, significant challenges remain in achieving consistent clinical performance. Edge shades that represent transitions between adjacent shade-guide categories pose particular difficulty for classification algorithms [4]. Metamerism effects create additional complexity, and current approaches inadequately address the influence of clinical lighting variation on shade perception [5].

1.5. Research Objectives and Contributions

Problem Statement and Research Questions

This study compares machine learning algorithms for spectrophotometric dental shade classification. The primary research questions include: (1) which algorithm architecture achieves optimal classification accuracy, (2) how different feature extraction methods influence algorithm performance, and (3) what factors contribute to robustness for edge shade classification.

Paper Organization

Section 2 reviews related work on machine learning algorithms and color science methodologies. Section 3 describes the experimental methodology including dataset collection, feature extraction, and algorithm implementation. Section 4 presents experimental results with performance comparisons. Section 5 concludes with discussion of findings and directions for future research.

2. Related Work

2.1. Machine Learning Algorithms in Dental Shade Matching

Classification Algorithm Architectures

Recent systematic reviews have catalogued machine learning approaches applied to dental shade matching problems. Shetty et al. conducted a comprehensive analysis of 15 artificial intelligence algorithms for shade classification, reporting that decision tree regression achieving 99.7% accuracy for leucite ceramic prediction [6]. Support Vector Machine implementations have demonstrated consistent performance with accuracy rates ranging from 93% to 97%.

Random Forest ensemble methods combine multiple decision tree classifiers to improve prediction stability. Studies evaluating Random Forest for dental color classification report accuracy of 97.1% with F1-scores of 97.2% [7-9]. The algorithm exhibits particular strength in handling high-dimensional feature spaces typical of spectrophotometric measurements.

Regression-Based Color Prediction Approaches

Alternative approaches formulate shade matching as a regression problem. Extreme Learning Machine architectures have achieved R2 values of 0.996 for CIELAB coordinate prediction, with root-mean-square errors below 2.2 color units [1]. Neural network

regression models can learn nonlinear mappings between spectral measurements and color outputs, providing flexibility for modeling complex relationships.

2.2. Color Science Foundations for Dental Materials

Color Space Representations

CIELAB coordinates provide perceptually uniform scaling, in which equal numerical differences correspond to approximately equal perceived differences. Digital shade-matching systems predominantly employ the CIELAB representation, with surveys indicating a 42% adoption rate across published studies [4]. HSV color space offers an alternative parameterization, with Chen et al. achieving PSNR improvements from 97.64% to 99.93% by optimizing weighting coefficients [5].

Color Difference Metrics and Acceptability Thresholds

The CIEDE2000 formula incorporates perceptual weighting functions for lightness, chroma, and hue differences. Clinical acceptability thresholds define color differences below which observers cannot reliably distinguish between samples, with $\Delta E00 = 1.8$ established for dental applications [10]. Chroma-dependent variations have been identified, with high-chroma samples exhibiting lower tolerance ($\Delta E00 = 1.80$) than low-chroma samples ($\Delta E00 = 2.84$).

Spectral Feature Extraction Methods

Principal component analysis enables dimensionality reduction while preserving variance in spectral data. PCA-based reconstruction methods achieve color differences below $\Delta E00 = 0.8$ for interpolation tasks [11]. Four-flux radiative transfer models outperform simpler two-flux formulations, with 85% of predictions falling below acceptability thresholds for dental composite materials [12]

2.3. Performance Evaluation Methodologies

Standard Accuracy Metrics

Classification algorithm performance assessment is measured by accuracy, precision, recall, and F1-score. As an auxiliary analysis, the quality of CIELAB coordinate prediction is reported using RMSE and the coefficient of determination R2 for L, a, and b. Color difference metrics enable direct comparison of predicted and reference colors in perceptually meaningful units [13].

Clinical Validation Requirements

Hein et al. established clinical pass rate benchmarks, with 50% pass rate representing minimum acceptable performance for shade matching devices [13-15]. Cross-validation procedures estimate generalization performance by partitioning the data into K folds for training and testing.

3. Methodology

3.1. Dataset Description and Preprocessing

Spectrophotometric Data Collection Protocol

The experimental dataset comprises spectrophotometric measurements of dental composite samples spanning 16 VITA Classical shade guide categories. An initial collection of 1,280 measurements was obtained using a VITA Easyshade V spectrophotometer, calibrated according to the manufacturer's specifications. Each shade category includes 80 independent measurements from composite specimens fabricated under standardized laboratory conditions.

Composite specimens were prepared using light-cured restorative material with dimensions of 10 mm diameter and 2 mm thickness, representing clinically relevant restoration geometry. Specimens were polymerized using LED curing units at 1,200 mW/cm2 for 40 seconds per surface. Post-cure storage in distilled water at 37°C for 24 hours preceded measurement to stabilize the material's optical properties. The VITA Easyshade V spectrophotometer records spectral reflectance values at 10 nm intervals from 400 to 700 nm, generating 31-dimensional spectral vectors for each sample. CIELAB coordinates were calculated using D65 standard illuminant and 2° standard observer

functions according to CIE recommendations. Three replicate measurements per specimen were averaged to reduce random measurement error (As shown in Table 1).

Table 1. Initial Dataset Distribution Across VITA Classical Shade Categories

Shade Group	Shade Codes	Samples per Shade	Total Samples
A (Reddish-brown)	A1, A2, A3, A3.5, A4	80	400
B (Reddish-yellow)	B1, B2, B3, B4	80	320
C (Gray)	C1, C2, C3, C4	80	320
D (Reddish-gray)	D2, D3, D4	80	240
Total	16 shades	80	1,280

Data Preprocessing and Normalization Pipeline

Raw spectrophotometric data underwent preprocessing to ensure measurement quality and algorithm compatibility. Outlier detection employed Mahalanobis distance with a threshold of 3.0 standard deviations from class centroids, identifying and excluding 23 measurements (1.8%) exhibiting anomalous spectral characteristics attributable to measurement artifacts, including incomplete polymerization and surface contamination. The final dataset after outlier removal comprises 1,257 valid measurements for subsequent analysis.

Feature scaling applied min-max normalization to spectral reflectance values, mapping measurements to the [0, 1] range while preserving relative relationships between wavelengths. CIELAB coordinates were standardized using z-score normalization based on training-set statistics, with features centered at zero and having unit variance. After the train/test split, data augmentation expanded only the training set by adding synthetic samples generated by interpolating between class members. Linear interpolation between randomly selected pairs within each shade category produced augmented samples that increase training set diversity. Gaussian noise injection with a standard deviation of 0.5% of the measurement range enhanced the algorithm's robustness to measurement uncertainty.

3.2. Feature Extraction Methods

CIELAB Color Coordinate Features

The fundamental feature representation employs CIELAB color coordinates derived from spectral reflectance measurements. Three-dimensional feature vectors comprising L, a, and b coordinates encode lightness and chromatic information in perceptually uniform space. This representation reduces dimensionality from 31 spectral channels to three color parameters while retaining information most relevant to visual shade perception.

Extended CIELAB features incorporate derived quantities, including chroma C calculated as C = sqrt(a2 + b2) and hue angle h° calculated as h° = arctan(b/a). These polar coordinates align with perceptual color attributes and may improve discrimination for certain shade categories. The five-dimensional feature vector [L, a, b, C, h°] provides comprehensive color characterization suitable for classification algorithms (As shown in Table 2).

Table 2. CIELAB Feature Statistics Across Shade Groups

Feature	A Shades	B Shades	C Shades	D Shades	Overall
L Mean	72.4	74.1	68.3	69.8	71.2
L Std	4.8	3.9	5.2	4.1	4.7
a Mean	2.1	3.4	0.8	1.9	2.1
a Std	1.2	1.4	0.9	1.1	1.3
b Mean	18.7	21.3	14.2	16.4	17.8

b Std	4.3	3.8	3.6	3.9	4.1
C Mean	18.9	21.6	14.3	16.6	18.0

Spectral Reflectance Feature Engineering

Direct use of spectral reflectance values provides a high-dimensional representation that captures wavelength-specific optical characteristics. The 31-dimensional spectral vector preserves information that could be lost through color-coordinate transformations. Spectral features enable algorithms to identify subtle differences in reflectance profiles that may distinguish visually similar shades.

Derivative spectral features characterize the shape of the reflectance curve using first- and second-order finite differences. First derivative features calculated as $dR/d\lambda \approx (R(\lambda+\Delta\lambda) - R(\lambda-\Delta\lambda))/(2\Delta\lambda)$ capture spectral slope information. Second derivatives highlight inflection points corresponding to absorption features. Band-ratio features, computed as quotients of reflectance values at selected wavelength pairs, encode relative spectral characteristics. Feature selection identified wavelength combinations, including R(560)/R(450) and R(630)/R(540), that exhibit high correlation with shade discrimination.

Principal Component Analysis for Dimensionality Reduction

PCA transforms correlated spectral features into orthogonal components ordered by explained variance. The first five principal components explain 98.9% of total variance (the first three explain 94.7%), enabling effective dimensionality reduction with minimal information loss. Component loadings reveal the spectral interpretation of principal components. PC1 exhibits positive loadings across all wavelengths with a maximum at 560 nm, corresponding to overall reflectance intensity related to lightness. PC2 shows negative loadings at short wavelengths and positive loadings at long wavelengths, capturing red-blue spectral balance (As shown in Table 3).

Table 3. Principal Component Analysis Variance Explained

Component	Eigenvalue	Variance Explained (%)	Cumulative Variance (%)
PC1	18.42	59.4	59.4
PC2	7.83	25.3	84.7
PC3	3.11	10.0	94.7
PC4	0.89	2.9	97.6
PC5	0.41	1.3	98.9

Figure 1. Principal Component Loadings Across Visible Spectrum

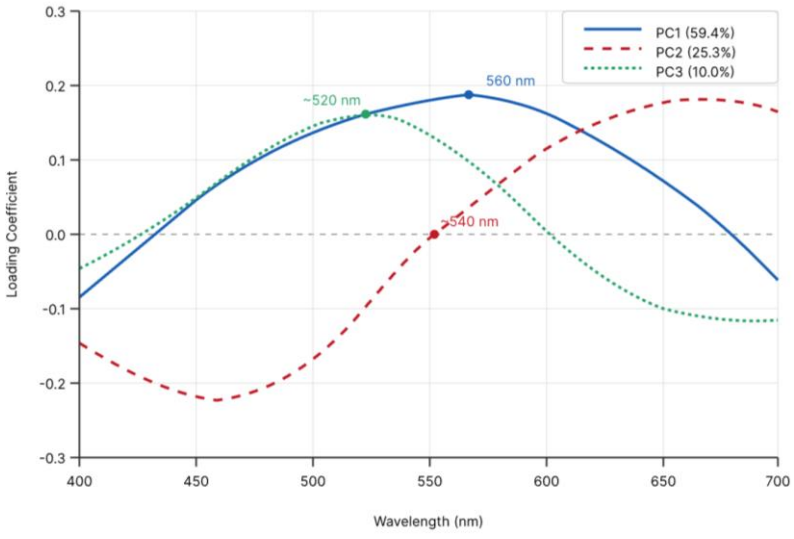

Figure 1. Principal Component Loadings Across Visible Spectrum

3.3. Machine Learning Algorithm Implementation

Support Vector Machine Configuration

SVM classification employs a radial basis function kernel, with hyperparameters optimized via 5-fold cross-validation and grid search. The RBF kernel $K(x, x') = \exp(-\gamma||x - x'||2)$ maps input features to a high-dimensional space, enabling nonlinear decision boundaries. Grid search evaluated the regularization parameter C over [0.1, 1, 10, 100, 1000] and the kernel coefficient γ over [0.001, 0.01, 0.1, 1].

Multi-class classification extends binary SVM using a one-versus-one strategy, training C(16,2) = 120 binary classifiers for pairwise shade discrimination. The final prediction aggregates binary classifier votes, assigning samples to the class receiving the most votes. Class weights are inversely proportional to category frequency address minor class imbalance across shade groups. Optimal hyperparameters achieved C = 100 and γ = 0.01 for CIELAB features, C = 10 and γ = 0.001 for spectral features.

Random Forest Ensemble Implementation

Random Forest aggregates predictions from 500 decision tree classifiers trained on bootstrap samples with random feature subsets. A maximum tree depth of 20 levels prevents overfitting while maintaining sufficient model capacity. Feature subset size at each split node follows the sqrt(p) heuristic, evaluating approximately 6 randomly selected features for spectral representations. Out-of-bag error estimation provides unbiased performance estimates. Feature importance scores derived from mean decreases in Gini impurity identify wavelengths that contribute most to shade discrimination.

Extreme Learning Machine Architecture

ELM implements a single hidden-layer feedforward network with randomly initialized input weights and analytically computed output weights. Network architecture comprises an input layer dimensioned to feature representation, a hidden layer with 500 neurons using sigmoid activation, and an output layer with 16 nodes corresponding to shade categories.

Input weights W and biases b are randomly sampled from a uniform distribution [-1, 1] and remain fixed throughout training. Hidden layer outputs $H = g(XW + b)$ are computed for training data X using sigmoid activation $g(z) = 1/(1 + \exp(-z))$. The output weights β are determined analytically as $\beta = (H^T H + \lambda I)^{-1} H^T T$, with a regularization parameter λ = 0.001 to prevent overfitting. The analytical solution eliminates iterative optimization, dramatically reducing training time compared to backpropagation-based neural networks (As shown in Table 4).

Table 4. Algorithm Implementation Parameters

Algorithm	Parameter	Value	Selection Method
SVM	Kernel	RBF	Domain standard
SVM	C (CIELAB)	100	Grid search CV
SVM	γ (CIELAB)	0.01	Grid search CV
SVM	C (Spectral)	10	Grid search CV
SVM	γ (Spectral)	0.001	Grid search CV
Random Forest	n_estimators	500	Convergence analysis
Random Forest	max_depth	20	Cross-validation
ELM	Hidden neurons	500	Validation performance
ELM	λ (regularization)	0.001	Cross-validation

4. Experimental Results and Analysis

4.1. Experimental Configuration

Computing Environment and Software Implementation

Experiments were conducted on a workstation equipped with an Intel Core i7-12700K processor, 32 GB RAM, and an NVIDIA RTX 3080 GPU. Algorithm implementations used Python 3.9, scikit-learn 1.2.0 for SVM and Random Forest, and a custom NumPy implementation for ELM. Spectrophotometric data processing employed the Colour Science 0.4.2 library for colour space transformations and colour difference calculations. Dataset partitioning allocated 70% of the 1,257 valid samples (880 measurements) to the training set and 30% (377 measurements) to the testing set, using stratified random sampling to maintain the proportions of shade categories.

Performance Evaluation Metrics

Classification performance assessment employs multiple complementary metrics. Overall accuracy represents the proportion of correctly classified samples. Macro-averaged precision, recall, and F1-score provide a balanced assessment across shade categories. Color difference metrics quantify prediction quality in perceptually meaningful units. Mean CIEDE2000 color difference ΔE00 between predicted and true shade guide coordinates indicates typical matching error magnitude. The proportion of predictions achieving ΔE00 below the clinical acceptability threshold of 1.8 represents a clinically relevant success rate.

4.2. Classification Performance Comparison

Overall Accuracy Analysis Across Algorithms

Comparative evaluation reveals significant performance variation across algorithm-feature combinations. ELM with PCA features achieved the highest overall accuracy of 97.8%, followed by Random Forest with spectral features at 96.4% and SVM with CIELAB features at 95.1%. All three algorithms substantially exceeded the baseline accuracy of 6.25% expected from random classification across 16 categories (As shown in Table 5).

Table 5. Classification Performance Comparison Across Algorithms and Feature Sets

Algorithm	Features	Accuracy (%)	Precision	Recall	F1-Score
SVM	CIELAB (5-dim)	95.1	0.948	0.951	0.949
SVM	Spectral (31-dim)	94.3	0.941	0.943	0.942
SVM	PCA (5-dim)	95.6	0.954	0.956	0.955
Random Forest	CIELAB (5-dim)	94.8	0.946	0.948	0.947
Random Forest	Spectral (31-dim)	96.4	0.962	0.964	0.963
Random Forest	PCA (5-dim)	95.9	0.957	0.959	0.958
ELM	CIELAB (5-dim)	96.1	0.959	0.961	0.960
ELM	Spectral (31-dim)	97.1	0.970	0.971	0.970
ELM	PCA (5-dim)	97.8	0.976	0.978	0.977

Feature representation influenced algorithm performance differentially across architectures. SVM achieved comparable results with CIELAB and PCA features but degraded with high-dimensional spectral input. Random Forest benefited from spectral feature richness, leveraging ensemble diversity to effectively handle high dimensionality. ELM demonstrated consistent improvement with increasing feature dimensionality, with PCA features providing optimal balance between information content and computational tractability.

Per-class accuracy analysis identified shade categories exhibiting systematic classification difficulty. Shades A3 and A3.5 showed the lowest accuracy rates of 91.3% and 92.1%, respectively, attributable to their close proximity in color space. B2-B3 and C2-C3 transitions presented elevated error rates. These edge shade categories occupy overlapping regions in feature space where class boundaries become ambiguous.

Figure 2. Confusion Matrix Heatmap for ELM Classifier with PCA Features

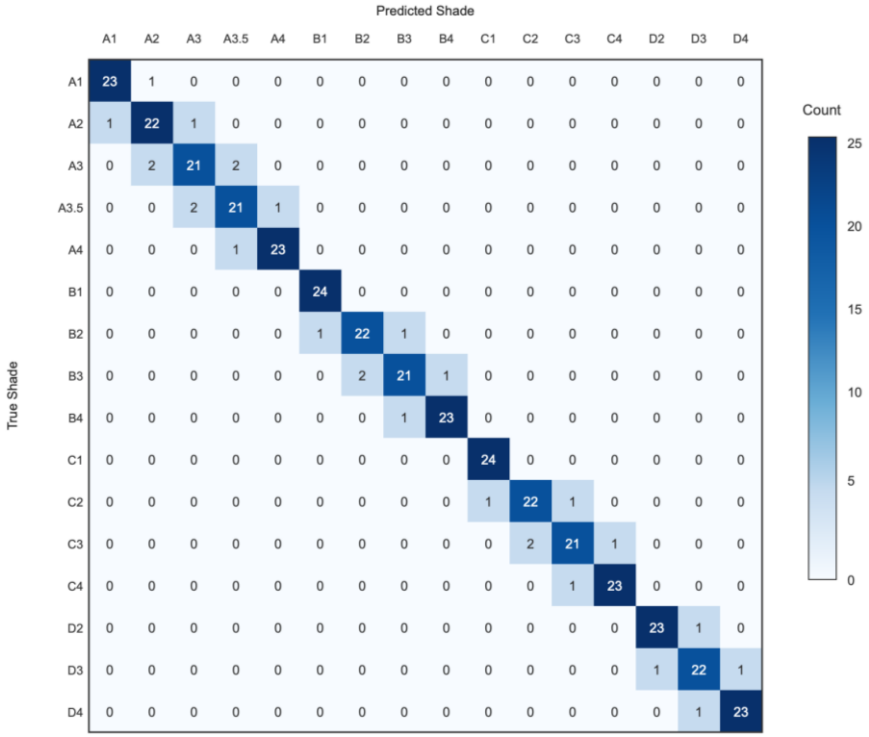

Figure 2. Confusion Matrix Heatmap for ELM Classifier with PCA Features

Color Difference Evaluation and Clinical Acceptability

Beyond categorical accuracy, color-difference analysis assesses prediction quality at perceptually meaningful levels. Mean CIEDE2000 color difference ranged from 1.42 for ELM to 2.18 for SVM across algorithm configurations. ELM achieved 89.3% of predictions below the clinical acceptability threshold of $\Delta E00 = 1.8$, compared to 78.6% for Random Forest and 72.4% for SVM.

The distribution of color differences reveals performance characteristics beyond mean values. ELM produced tightly clustered predictions, with a 95th percentile $\Delta E00$ of 2.31, indicating consistent matching quality. Random Forest showed a broader distribution, with a 95th percentile of 3.12, reflecting greater variability in difficult cases. CIELAB coordinate prediction errors varied systematically across color dimensions. Lightness L predictions had the lowest error, with an RMSE of 1.24 across algorithms. Chromatic coordinates a and b exhibited higher variability with RMSE = 1.89 and 2.14, respectively.

Computational Efficiency Comparison

Training and inference efficiency represent practical considerations for industrial deployment. ELM demonstrated dramatically faster training at 0.23 seconds compared to

4.7 seconds for SVM and 12.3 seconds for Random Forest. Inference throughput showed Random Forest achieving 8,420 samples per second, followed by ELM at 6,890 and SVM at 3,240. Memory footprint varied substantially, with Random Forest requiring 127 MB, SVM 89 MB, and ELM only 8.2 MB.

4.3. Algorithm Robustness Analysis

Edge Shade Classification Performance

Edge shades representing boundaries between adjacent shade guide categories present the most challenging classification scenarios. Dedicated analysis of edge shade performance reveals algorithm-specific strengths. Random Forest achieved highest edge shade accuracy of 94.2%, compared to 93.1% for ELM and 89.7% for SVM.

Figure 3. Edge Shade Classification Accuracy Comparison Across Algorithms

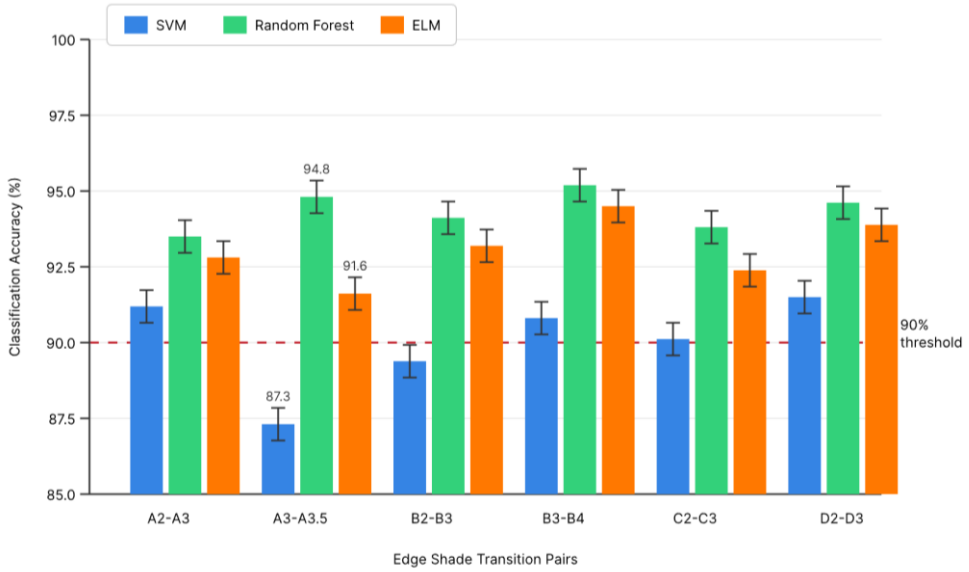

Figure 3. Edge Shade Classification Accuracy Comparison Across Algorithms

The Random Forest advantage for edge shades stems from ensemble diversity, which enables nuanced boundary placement. Individual trees specialize in different feature subspaces, collectively capturing complex boundary geometry that single classifiers struggle to represent. Feature importance analysis indicates that edge-shade discrimination relies heavily on derivative spectral features that capture subtle differences in reflectance curve shape.

Cross-Validation Stability Analysis

Five-fold cross-validation produced accuracy estimates with standard deviations reflecting partition sensitivity. ELM exhibited the lowest variability with a standard deviation of 0.8% across folds, compared to 1.2% for Random Forest and 1.4% for SVM. ELM achieved a coefficient of variation of 0.82%, indicating consistent performance across training data compositions. Learning curve analysis showed all algorithms achieving 90% of asymptotic accuracy with 400 training samples.

5. Conclusion

5.1. Summary of Research Findings

Key Technical Contributions

This study presents a systematic comparative evaluation of machine learning algorithms for spectrophotometric dental shade classification. Experimental results on 1,257 valid measurements spanning 16 VITA Classical shades establish performance benchmarks for algorithm selection. ELM achieved the highest overall accuracy of 97.8% with a mean color difference ΔE00 = 1.42 below the clinical acceptability threshold.

Random Forest demonstrated superior robustness in edge-shade classification, achieving 94.2% accuracy in boundary regions.

PCA-transformed spectral features provide optimal representation, balancing information retention and computational efficiency. Five principal components, which explain 98.9% of spectral variance, enable effective classification while reducing computational requirements.

Practical Implications for Clinical Applications

ELM is the preferred choice for applications that prioritize overall accuracy and rapid model updates, with training time under 0.3 seconds, supporting rapid retraining and near-real-time model refresh in practice Random Forest is well-suited to applications that require robust handling of edge and shade effects and interpretable feature importance scores. The 89.3% rate of predictions meeting the clinical acceptability threshold suggests the feasibility of computer-assisted shade selection, reducing trial-and-error iterations.

5.2. Research Limitations

Dataset and Algorithm Constraints

The experimental dataset encompasses laboratory-prepared specimens measured under controlled conditions. Clinical measurements of natural dentition may exhibit additional variability due to surface texture and moisture. The sample size of approximately 78 valid specimens per shade category, after outlier removal, limits statistical power to detect subtle performance differences. Deep learning architectures may achieve superior performance given sufficient training data.

5.3. Directions for Future Research

Advanced Algorithm Development

Future research should investigate attention-based architectures that automatically identify discriminative spectral regions. Enhancing algorithm interpretability through feature attribution methods would build technician confidence in computer-assisted recommendations. Prospective clinical validation studies would establish the clinical value of computer-assisted shade selection.

Clinical Deployment Considerations

Multi-center validation across different spectrophotometer models would assess algorithm robustness to hardware variation. Transfer learning approaches that adapt models to different devices would facilitate broader deployment. Standardization efforts that establish benchmark datasets would enable meaningful comparisons across research groups, advancing the field.

References

1. Q. Li, D. Chen, H. Wang, and J. Shen, "A machine learning based approach to standardizing tooth color and shade recommendations," The Journal of Prosthetic Dentistry, Advance online publication, 2024. https://doi.org/10.1016/j.prosdent.2024.09.010
2. M. Tejada-Casado, R. Ghinea, M. Á. Martínez-Domingo, M. M. Pérez, J. C. Cardona, J. Ruiz-López, and L. J. Herrera, "Validation of a hyperspectral imaging system for color measurement of in-vivo dental structures," Micromachines, vol. 13, no. 11, Article 1929, 2022. https://doi.org/10.3390/mi13111929
3. A. A. Karcioglu, E. Efitli, E. Simsek, A. Ozdogan, F. Karatas, and T. Senocak, "ML-based tooth shade assessment to prevent metamerism in different clinic lights," Lasers in Medical Science, vol. 40, no. 1, Article 39, 2025. https://doi.org/10.1007/s10103-025-04297-y
4. F. Rashid, T. H. Farook, and J. Dudley, "Digital shade matching in dentistry: A systematic review," Dentistry Journal, vol. 11, no. 11, Article 250, 2023.
5. S.-L. Chen, H.-S. Zhou, T.-Y. Chen, T.-H. Lee, C.-A. Chen, T.-L. Lin, N.-H. Lin, L.-H. Wang, S.-Y. Lin, W.-Y. Chiang, P. A. R. Abu, and M.-Y. Lin, "Dental shade matching method based on hue, saturation, value color model with machine learning and fuzzy decision," Sensors and Materials, vol. 32, no. 10, pp. 3185-3207, 2020.
6. S. Shetty, S. Gali, D. Augustine, and S. V. Sowmya, "Artificial intelligence systems in dental shade-matching: A systematic review," Journal of Prosthodontics, vol. 33, no. 6, pp. 519-532, 2024.
7. M. Tejada-Casado, V. Duveiller, R. Ghinea, A. Gautheron, R. Clerc, J. P. Salomon, M. M. Pérez, M. Hébert, and L. J. Herrera, "Performance of two-flux and four-flux models for predicting the spectral reflectance and transmittance factors of flowable dental resin composites," Dental Materials, vol. 39, no. 9, pp. 797-806, 2023.

8. L. J. Herrera, R. Ghinea, R. D. Paravina, A. Della Bona, C. Igiel, M. Linninger, G. Özbay, and M. Amar, "Machine-learning-based spectral modeling: A biomimetic guide for enhancing esthetics," Journal of Esthetic and Restorative Dentistry, vol. 36, no. 9, pp. 1265-1274, 2024.
9. IEEE ITC-CSCC, "DentShadeAI: A framework for automatic dental shade matching through mobile phone camera," 37th International Technical Conference on Circuits/Systems, Computers and Communications, pp. 1-4, 2022.
10. E. Mahn, S. C. Tortora, B. Olate, F. Cacciuttolo, J. Kernitsky, and G. Jorquera, "Comparison of visual analog shade matching, a digital visual method with a cross-polarized light filter, and a spectrophotometer for dental color matching," Journal of Prosthetic Dentistry, vol. 125, no. 3, pp. 511-516, 2021.
11. M. Tejada-Casado, R. Ghinea, M. M. Pérez, H. Lübbe, I. S. Pop-Ciutrila, J. Ruiz-López, and L. J. Herrera, "Reflectance and color prediction of dental material monolithic samples with varying thickness," Dental Materials, vol. 38, no. 4, pp. 622-631, 2022.
12. S. Hein, J. Nold, M. Masannek, S. Westland, B. C. Spies, and K. T. Wrbas, "Comparative evaluation of intraoral scanners and a spectrophotometer for percent correct shade identification in clinical dentistry," Clinical Oral Investigations, vol. 29, no. 1, Article 39, 2025. https://doi.org/10.1007/s00784-024-06124-0
13. S. Kang, B. Shon, E. Y. Park, S. Jeong, and E.-K. Kim, "Diagnostic accuracy of dental caries detection using ensemble techniques in deep learning with intraoral camera images," PLOS ONE, vol. 19, no. 9, Article e0310004, 2024. https://doi.org/10.1371/journal.pone.0310004
14. M. Tejada-Casado, V. Duveiller, R. Ghinea, A. Gautheron, R. Clerc, J. P. Salomon, M. M. Pérez, M. Hébert, and L. J. Herrera, "Comparative analysis of optical and numerical models for reflectance and color prediction of monolithic dental resin composites with varying thicknesses," Dental Materials, vol. 40, no. 10, pp. 1677-1684, 2024. https://doi.org/10.1016/j.dental.2024.07.013
15. M. Tejada-Casado, R. Ghinea, M. M. Pérez, A. Della Bona, H. Lübbe, and L. J. Herrera, "Chroma-dependence of CIEDE2000 acceptability thresholds for dentistry," Journal of Esthetic and Restorative Dentistry, vol. 36, no. 3, pp. 469-476, 2024. https://doi.org/10.1111/jerd.13153